Supporting information for

Lanthanum-Mediated Single-Atom Dispersion of Ir and Dynamic Oxygen Replenishment in Acidic Water Oxidation

Chen Cao [a b c], Shirui Cui[a], Feng Shi [b c], Yanqin Li [a], Chunyang Zhao [a], Wei Hu [a], Zelong Li [a] *, Yu Tang [a] *

[a]Key Laboratory of Advanced Catalysis, Gansu Province, State Key Laboratory of Applied Organic Chemistry, Key Laboratory of Nonferrous Metal Chemistry and Resources Utilization of Gansu Province, College of Chemistry and Chemical Engineering, Lanzhou University, Lanzhou, Gansu 730000, China

[b]State Key Laboratory of Low Carbon Catalysis and Carbon Dioxide Utilization Lanzhou Institute of Chemical Physics, Chinese Academy of Sciences No.18, Tianshui Middle Road, Lanzhou, 730000, China

[c]University of Chinese Academy of Sciences, Beijing 100049, China

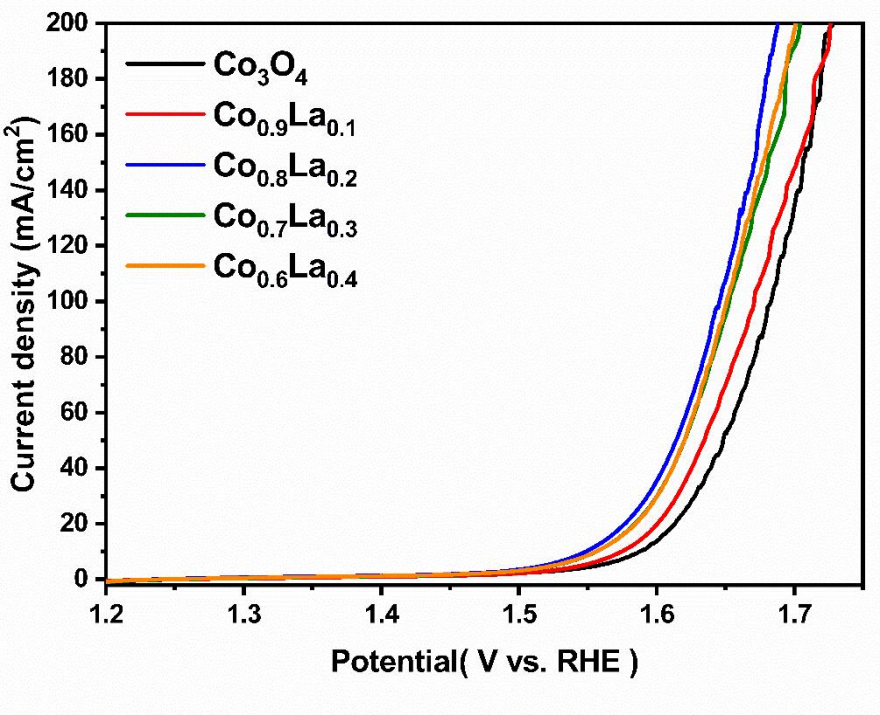

Fig. S1. LSV curves of catalysts with different La contents.

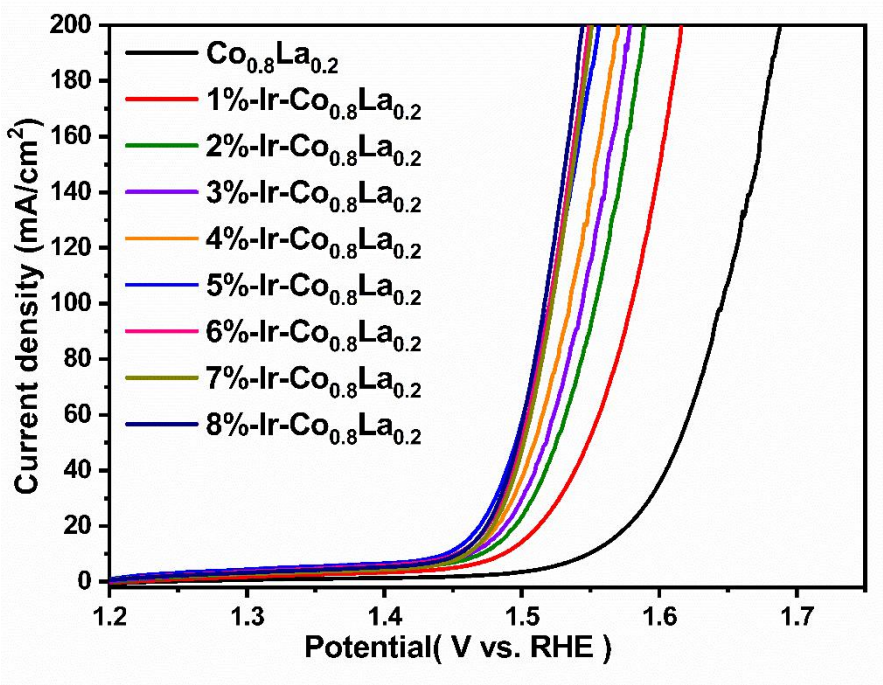

Fig. S2. LSV curves of $Co_{0.8}La_{0.2}$ impregnated with different molar ratios of iridium.

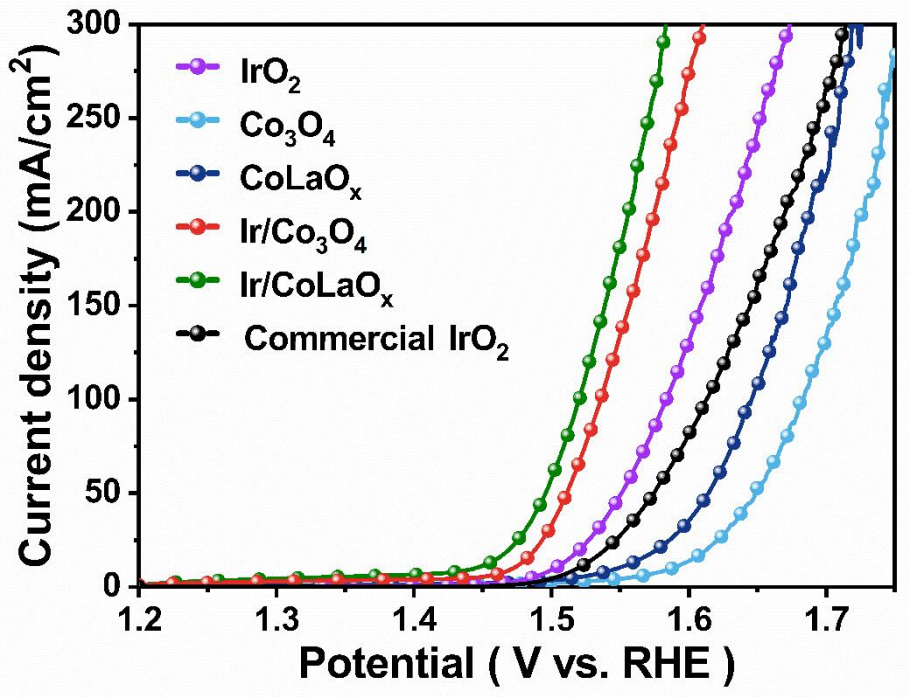

Fig. S3. LSV curves of different catalysts.

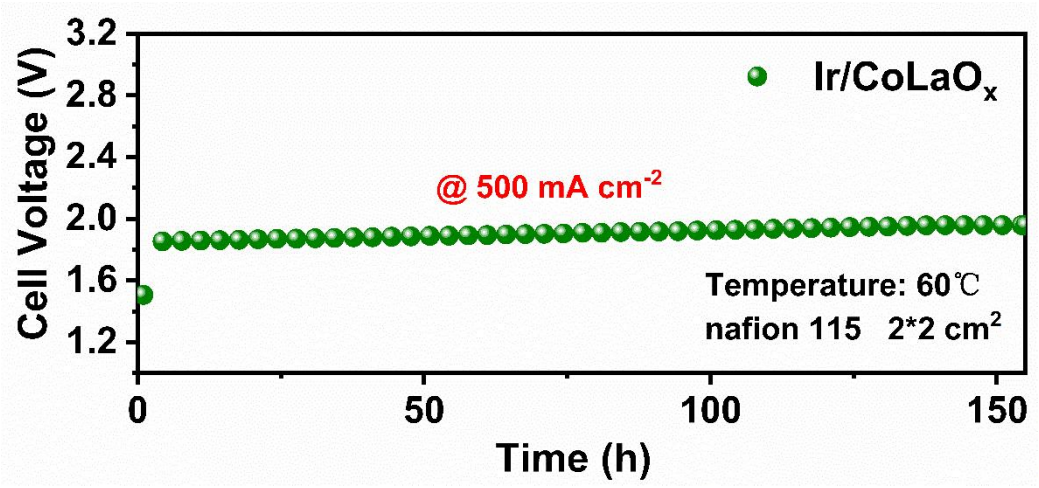

Fig. S4. V-t curve of the PEM cell for Ir/CoLaO$_x$, operating at 500 mA cm^{-2}, 60 °C, and ambient pressure.

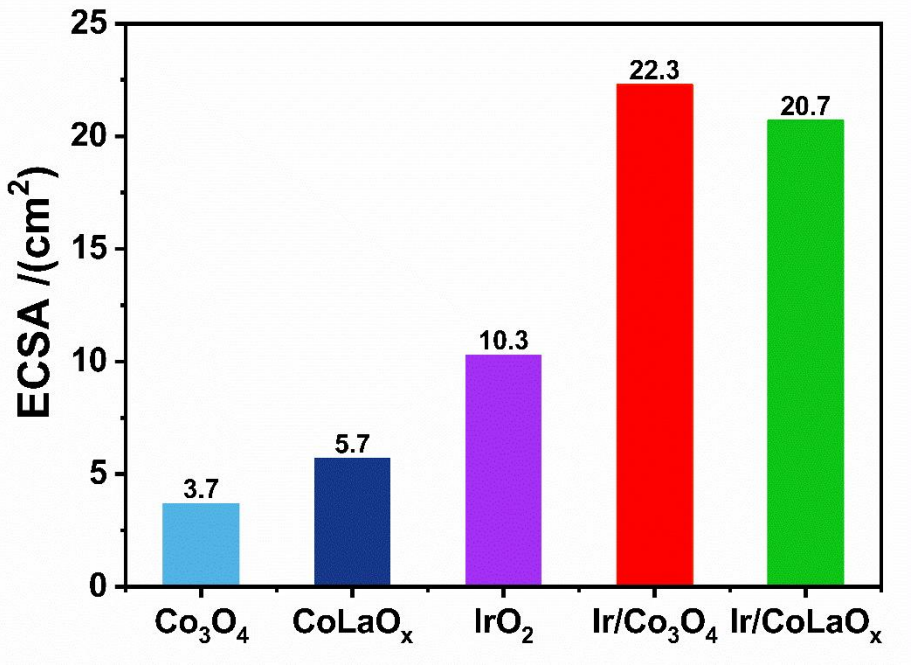

Fig. S5. ECSA of Co_3O_4, $CoLaO_x$, IrO_2, Ir/Co_3O_4 and Ir/$CoLaO_x$.

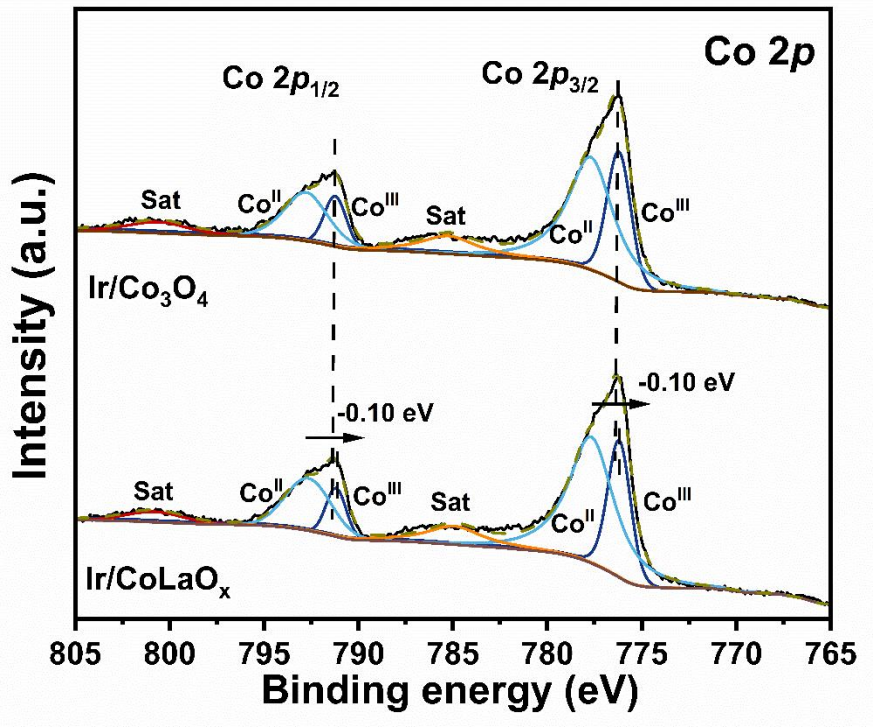

Fig. S6. XPS spectra of Co 2*p* for $Ir/CoLaO_x$ and Ir/Co_3O_4.

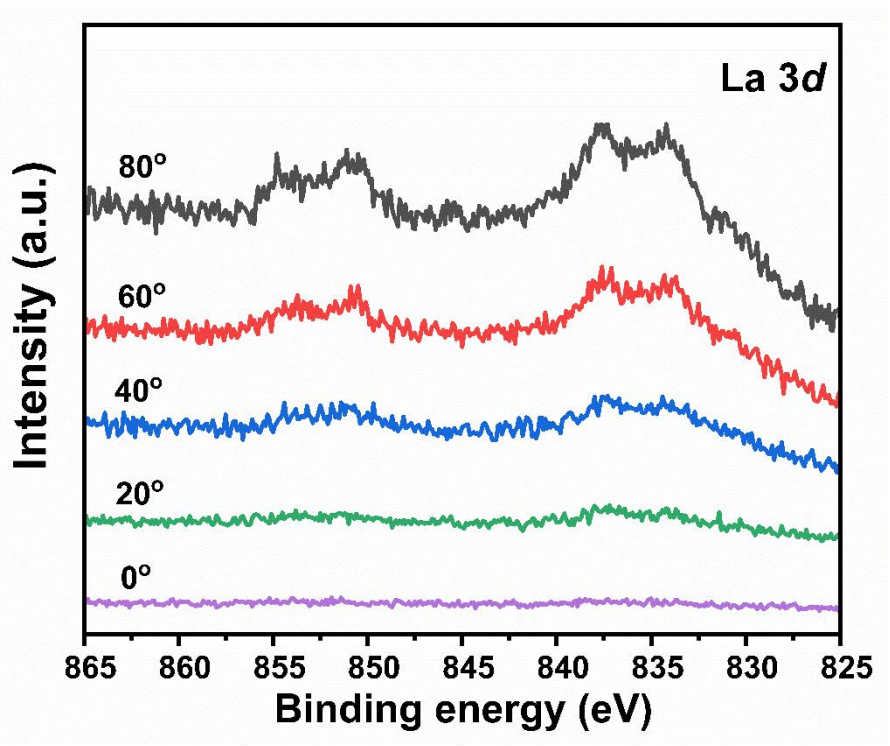

Fig. S7. Angle-Resolved XPS Spectra of La 3d Orbital

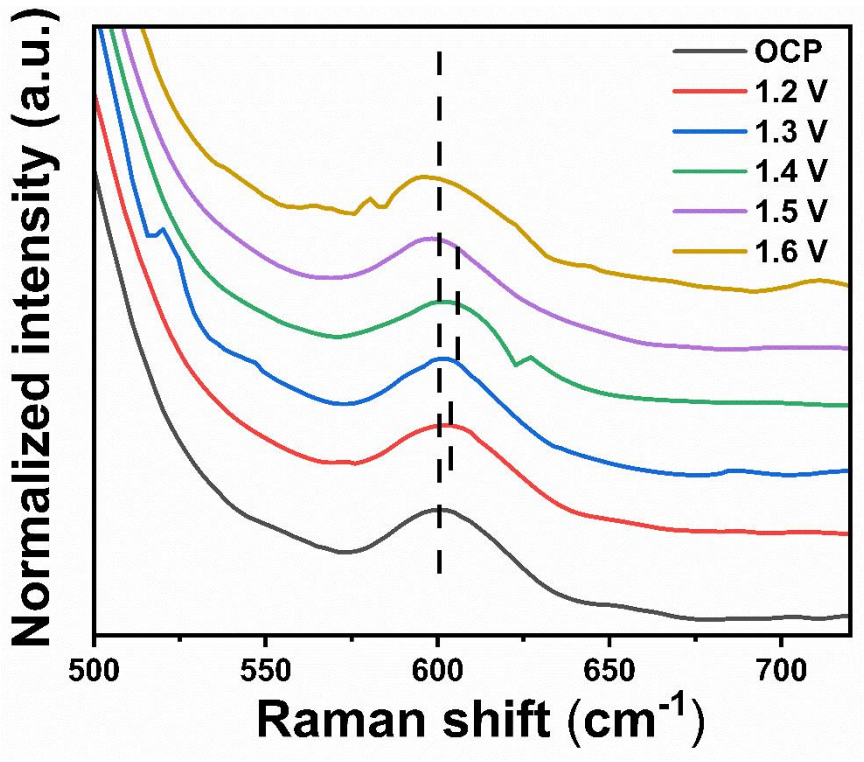

Fig. S8. In-situ electrochemical Raman spectroscopy of Ir/CoLaO$_x$

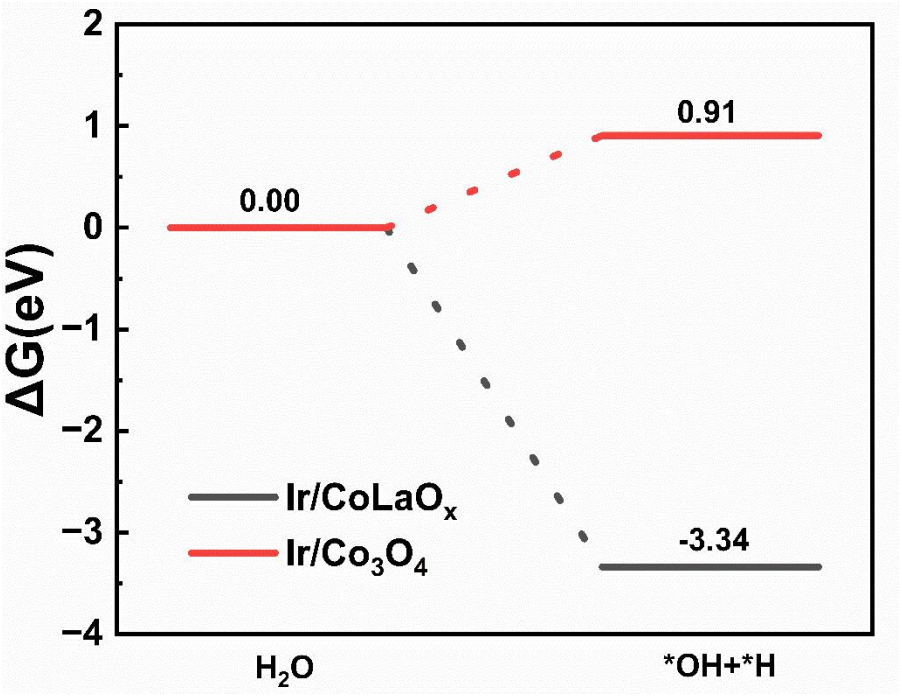

Fig. S9. DFT-calculated reaction coordinate for the energetics associated with the oxygen-vacancy refilling process by water on the two catalysts

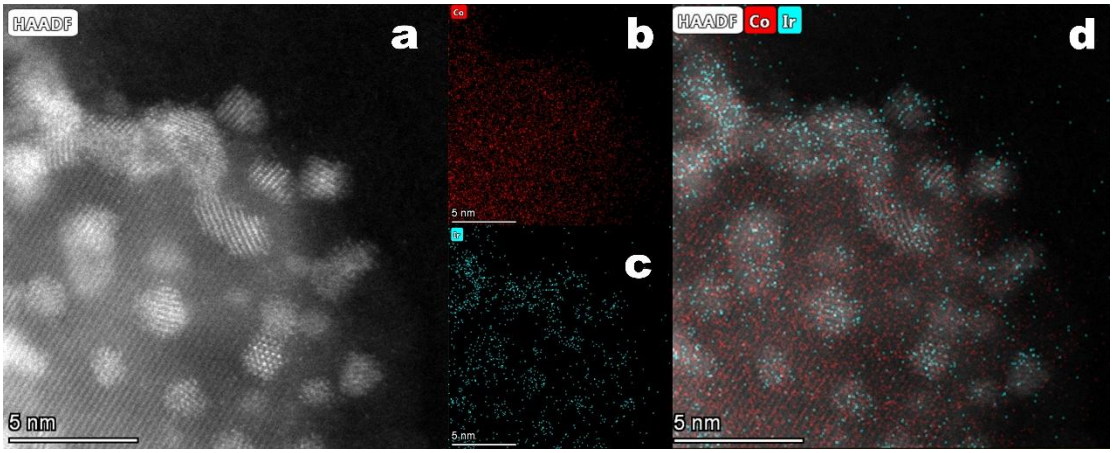

Fig. S10. (a) AC-HADDF-STEM image of Ir/Co_3O_4. (b) (c) (d) EDS elemental mappings of Ir/Co_3O_4.

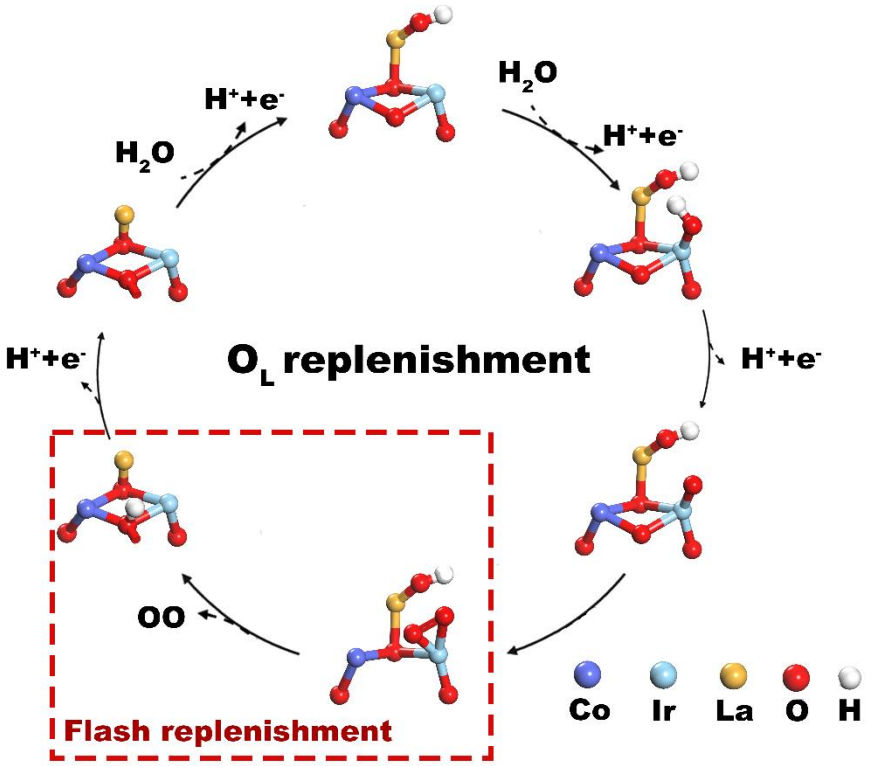

Figure S11. Schematic illustration of the electrochemical interface during water oxidation.

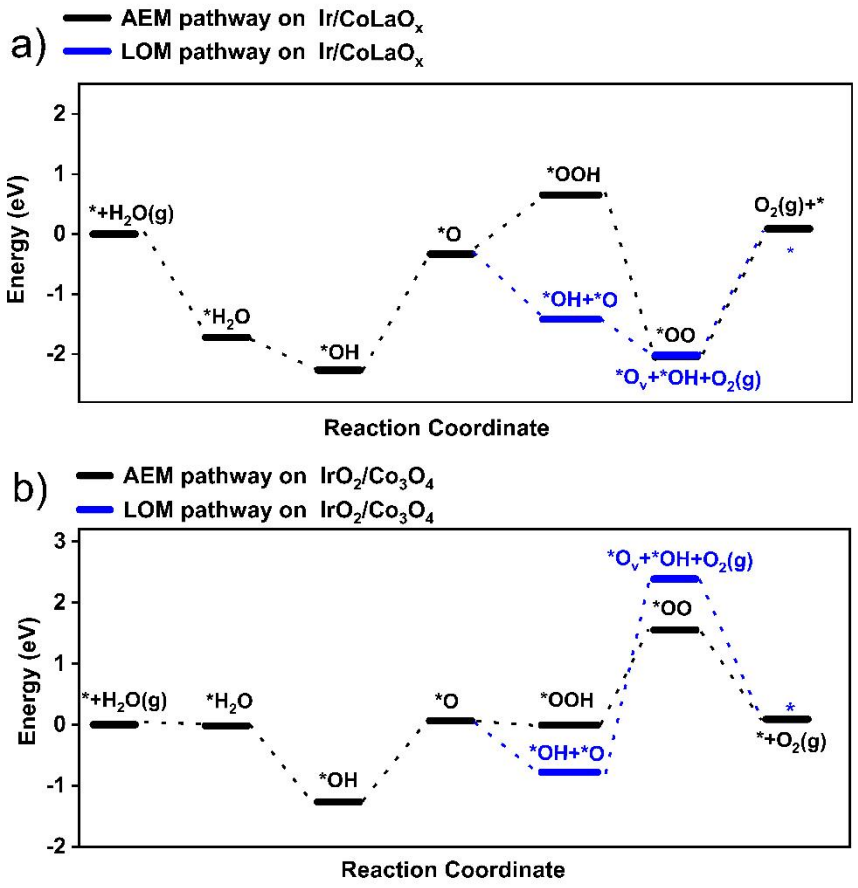

Figure S12. DFT-calculated reaction coordinate for all steps of the LOM and AEM over a) Ir/CoLaO$_x$ and b) IrO$_2$/Co$_3$O$_4$

Table S1. Parameters used in EXAFS fittings.

Sample	Shell	Bond length (Å)	Coordination Number	σ^2 (Å^2)	E0 shift (eV)	R-factor
Co_3O_4	Co-O	1.92±0.01	5.6±0.6	0.003±0.001	-4.0±1.5	0.008
	Co-Co	2.87±0.01	5.7±0.5	0.003±0.002		
	Co-Co	3.38±0.02	6.3±1.1	0.009±0.003		
IrO_2	Ir-O	2.02±0.01	5.5±0.3	0.006±0.001	8.2±0.7	0.008I
	Ir-Ir	3.14±0.02	4.2±0.3	0.011±0.004		
Ir/Co_3O_4	Co-O	1.93±0.01	5.6±0.7	0.003±0.001	3.2±1.7	0.012
	Co-Co	2.87±0.01	5.7±1.1	0.005±0.002		
	Co-Co	3.39±0.02	5.6±0.8	0.009±0.003		
	Ir-O	2.03±0.02	5.7±0.7	0.006±0.003	8.3±2.2	0.013
	Ir-Ir(Co)	2.85±0.02	3.1±0.2	0.007±0.005		
$CoLaO_x$	Co-O	1.93±0.01	5.4±0.6	0.006±0.001	3.2±1.5	0.008
	Co-Co	2.88±0.01	5.7±0.9	0.008±0.002		
	Co-Co	3.39±0.01	5.7±0.4	0.011±0.003		
$Ir/CoLaO_x$	Co-O	1.92±0.01	5.4±0.6	0.004±0.001	-2.9±1.8	0.009
	Co-Co	2.87±0.01	5.7±0.5	0.007±0.002		
	Co-Co	3.37±0.02	5.3±0.9	0.011±0.003		
	Ir-O	2.01±0.01	5.5±0.4	0.007±0.002	9.0±1.9	0.020
	Ir-Ir(Co)	2.78±0.04	2.5±0.2	0.014±0.005		

[a]. The value of the amplitude reduction factor (S_0^2) lines between 0.7 and 1; [b]. Bond length is the interactomic distance; [c]. CN is the coordination number; [d]. σ^2 is Debye-Waller factor (a measure of thermal and static disorder in absorber scatter distance); [e]. E_0 shift is edge-energy shift (the difference between the zero kinetic energy value of the sample and that of the theoretical model); [f]. R factor is used to value the goodness of the fitting.